

Supporting Information

Mechanistic insights into diversified photoluminescent behaviours of BF₂ complexes of *N*-benzoyl 2-aminobenzothiazoles

He Zheng,^a Yan-Xue Li,^a Wen-Chao Xiong,^a Xing-Cong Wang,^a Shan-Shan Gong,^a Shouzhi Pu,^{*b}
Rongwei Shi^{*c} and Qi Sun^{*a}

^a Jiangxi Key Laboratory of Organic Chemistry, Jiangxi Science and Technology Normal University, 605 Fenglin
Avenue, Nanchang, 330013, PR China

^b Department of Ecology and environment, Yuzhang Normal University, Nanchang 330103, PR China

^c School of Material and Chemical Engineering, Tongren University, Tongren, 554300, PR China

E-mails: pushouzhi@tsinghua.org.cn; njutshirongwei@163.com; sunqi@jxstnu.edu.cn

Table of contents

1. General methods	Page S2–S3
2. Synthetic procedures and characterization	Page S3–S4
3. Photophysical properties (Fig. S1–S5)	Page S5–S6
4. Theoretical calculations (Fig. S6–S9 and Table S1–S5)	Page S6–S9
5. Crystallographic analysis (Fig. S10 and Table S6)	Page S10–S11
6. NMR spectra (Fig. S11–S22)	Page S12–S17

1. General methods

1.1 Synthesis of **BFBB-1-4**

All chemical reagents and solvents were obtained from commercial suppliers. All reactions were performed in commercial AR grade solvents and monitored by thin layer chromatography on plates coated with 0.25 mm silica gel 60 F₂₅₄. TLC plates were visualized by UV irradiation. Flash column chromatography employed silica gel (particle size 32–63 μm). NMR spectra were obtained with a Bruker AV-400 and a Bruker AV-500 instrument with chemical shifts reported in parts per million (ppm, δ) and referenced to CDCl_3 . IR spectra were recorded on a Bruker Vertex-70 spectrometer. Low-resolution and high-resolution mass spectra were obtained with a Bruker amaZon SL mass spectrometer and a Bruker Dalton micrOTOF-Q II spectrometer, respectively, and reported as m/z . Melting points were measured on a Tech X-4 melting point apparatus and uncorrected.

1.2 UV-Vis and fluorescence spectrometry

Absorbance spectra of solution samples ($1 \times 10^{-6} \sim 1 \times 10^{-5}$ M) were recorded on an Agilent 8453 spectrophotometer. Absorbance spectra of solid samples were recorded on a PerkinElmer Lambda 750 spectrophotometer. Fluorescence spectra of solution ($1 \times 10^{-6} \sim 1 \times 10^{-5}$ M) and solid samples were recorded on a Hitachi F-4600 fluorescence spectrophotometer. Optical length of the quartz cell was 10 mm. Fluorescence quantum yields of solution (1×10^{-6} M) and solid samples were determined on a Hamamatsu absolute PL quantum yield spectrometer C11347. Fluorescence lifetimes were recorded on a Hamamatsu compact fluorescence lifetime spectrometer C11367.

1.3 Theoretical calculations

Ground- and excited-state geometrical optimization and vertical excitation of all BFAB compounds were carried out at the B3LYP/6-311G(d,p) level of theory implemented on the Gaussian 16 package. Polarizable continuum model (PCM) with corrected linear response (cLR) formalism were employed for solvent effect. MECI calculations were performed by using SF-TDDFT method with BHHLYP functional and 6-311G(d,p) basis set implanted in GAMESS program. The solid-phase computational model for **BFBB-1**, **2**, and **4** were set up based on their X-ray crystal structure. The QM/MM calculations were carried out by the two-layered ONIOM method with the central molecule (in “capped stick” model) as the high-layer QM part and the surrounding molecules (in “line” model) as the low-layer MM part. The initial models consist of 102 molecules (3060 atoms) for **BFBB-1**, 108 molecules (3672 atoms) for **BFBB-2**, 120 molecules (4560 atoms) for **BFBB-4**, respectively. One central molecule (30 atoms for **BFBB-1**, 34 atoms for **BFBB-2**, and 38 atoms for **BFBB-3**) is defined as the QM region. The universal force field (UFF) was applied in the MM section, and the electrostatic embedding scheme was adopted in the QM/MM treatment. The optimized ground- and excited-state geometries in QM region were optimized with B3LYP/6-311G(d,p) basis set.

1.4 DLS measurement

Particle size distribution was measured on a Nano Brook 90 Plus instrument equipped with a diode laser as a light source ($\lambda = 640.0$ nm). The scattered light from the sample solution was detected using a fixed angle (90°).

1.5 X-ray crystallographic analysis

Data collection for X-ray crystal analysis was performed on a Bruker Smart APEX-II single

crystal X-ray diffractometer using graphite monochromated Mo-K α radiation ($\lambda = 0.71073 \text{ \AA}$) at 296 K. The single crystals of **BFBB-1**, **2** and **4** were obtained by recrystallization from specific solvent system as mentioned in the Section 2.3. The structures were solved by direct methods using SHELXL crystallographic software package. Crystallographic data were deposited in the Cambridge Crystallographic Data Centre (CCDC): Nos. 2295395, 2295401, and 2295402.

2. Synthetic procedures and characterization of BFBB-1–4

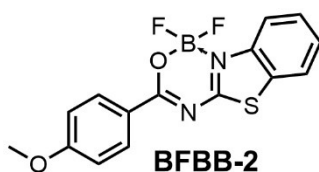
2.1 General synthetic procedures for BFBB-1–4

To a solution of *N*-benzoyl 2-aminobenzothiazoles (1.0 mmol) and *N,N*-diisopropylethylamine (5.0 mmol) in anhydrous dichloromethane (10 mL) was added BF₃·OEt₂ (10.0 mmol). The reaction was stirred at ambient temperature under argon for 5–10 h. The reaction solution was washed with brine (10 mL), dried over anhydrous Na₂SO₄, and evaporated under vacuum. Flash column chromatography (PE/EA = 8:1) afforded **BFBB-1–4** in pure form.

2.2 Characterization of BFBB-1–4

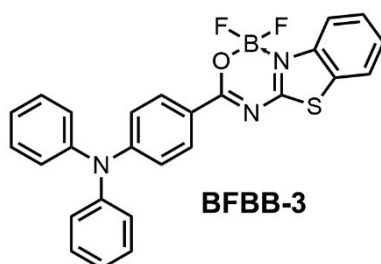


*1,1-Difluoro-3-phenyl-1H-1 λ^4 ,2 λ^3 -benzo[4,5]thiazolo[3,2-*c*][1,3,5,2]oxadiazaborinine (BFBB-1).* The reaction of *N*-(benzo[*d*]thiazol-2-yl)benzamide (254 mg, 1.0 mmol) afforded **BFBB-1** (173 mg, 57%) as a white solid; mp 201–202 °C. ¹H NMR (400 MHz, CDCl₃): δ 8.40 (d, *J* = 8.0 Hz, 2H), 8.08 (d, *J* = 8.4 Hz, 1H), 7.82 (d, *J* = 8.0 Hz, 1H), 7.67–7.60 (m, 2H), 7.54–7.48 (m, 3H) ppm; ¹³C NMR (100 MHz, CDCl₃): δ 174.3, 168.8, 140.3, 134.6, 131.2, 130.7 ($\times 2$), 128.9 ($\times 2$), 128.6, 127.4, 126.7, 122.3, 118.9 ppm; ¹⁹F NMR (470 MHz, CDCl₃): δ -135.76 (d, *J* = 10.3 Hz), -135.80 (d, *J* = 10.3 Hz); IR (KBr): ν_{\max} 3436, 3068, 1588, 1510, 1480, 1441, 1386, 1335, 1244, 1136, 1059, 918, 806, 760 cm⁻¹; LRMS (ESI+): *m/z* calcd for C₁₄H₁₀BF₂N₂OS [M+H]⁺ 303.1; found 303.1.

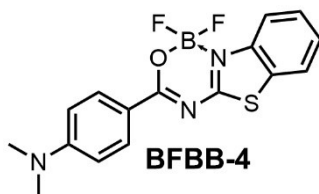


*1,1-Difluoro-3-(4-methoxyphenyl)-1H-1 λ^4 ,2 λ^3 -benzo[4,5]thiazolo[3,2-*c*][1,3,5,2]oxadiazaborinine (BFBB-2).* The reaction of *N*-(benzo[*d*]thiazol-2-yl)-4-methoxybenzamide (284 mg, 1.0 mmol) afforded **BFBB-2** (183 mg, 55%) as a yellow solid; mp 221–222 °C. ¹H NMR (400 MHz, CDCl₃): δ 8.36 (d, *J* = 8.8 Hz, 2H), 8.05 (t, *J* = 5.6 Hz, 1H), 7.78 (d, *J* = 8.0 Hz, 1H), 7.59 (t, *J* = 8.4 Hz, 1H), 7.47 (t, *J* = 8.0 Hz, 1H), 6.99 (d, *J* = 8.8 Hz, 2H), 3.91 (s, 3H) ppm; ¹³C NMR (100 MHz, CDCl₃): δ 174.3, 168.4, 165.3, 140.4, 133.1 ($\times 2$), 128.4, 127.2, 126.4, 123.5, 122.3, 118.7, 114.3 ($\times 2$), 55.8 ppm; ¹⁹F NMR (470 MHz, CDCl₃): δ -136.37

(d, $J = 9.4$ Hz), -136.42 (d, $J = 9.4$ Hz); IR (KBr): ν_{\max} 3450, 2949, 1605, 1583, 1485, 1386, 1241, 1135, 1021, 927, 836, 760 cm^{-1} ; LRMS (ESI+): m/z calcd for $\text{C}_{15}\text{H}_{12}\text{BF}_2\text{N}_2\text{O}_2\text{S}$ $[\text{M}+\text{H}]^+$ 333.1; found 333.1.



4-(1,1-Difluoro-1H-1 λ^4 ,2 λ^3 -benzo[4,5]thiazolo[3,2-c][1,3,5,2]oxadiazaborinin-3-yl)-N,N-diphenylaniline (**BFBB-3**). The reaction of *N*-(benzo[*d*]thiazol-2-yl)-4-(diphenylamino)benzamide (105 mg, 0.25 mmol) afforded **BFBB-3** (55 mg, 47%) as a yellow solid; mp 242–243 °C, ^1H NMR (400 MHz, CDCl_3): δ 8.19 (d, $J = 8.8$ Hz, 2H), 8.01 (d, $J = 8.0$ Hz, 1H), 7.76 (d, $J = 8.0$ Hz, 1H), 7.58–7.52 (m, 1H), 7.44 (d, $J = 8.8$ Hz, 1H), 7.36 (t, $J = 8.0$ Hz, 4H), 7.37–7.17 (m, 6H), 6.99 (d, $J = 8.8$ Hz, 2H) ppm; ^{13}C NMR (100 MHz, CDCl_3): δ 174.1, 168.1, 153.8, 146.3 ($\times 2$), 140.5, 132.4 ($\times 2$), 129.9 ($\times 4$), 128.3, 127.1, 126.6 ($\times 4$), 126.2, 125.5 ($\times 2$), 122.2, 119.2 ($\times 3$), 118.5 ppm; ^{19}F NMR (470 MHz, CDCl_3): δ -135.38 (d, $J = 10.7$ Hz), -135.43 (d, $J = 10.7$ Hz); IR (KBr): ν_{\max} 3441, 2963, 1612, 1589, 1457, 1423, 1385, 1338, 1181, 1130, 1055, 921, 876, 758 cm^{-1} ; HRMS (ESI+): m/z calcd for $\text{C}_{26}\text{H}_{19}\text{BF}_2\text{N}_3\text{OS}$ $[\text{M}+\text{H}]^+$ 470.1304; found 470.1308.



4-(1,1-Difluoro-1H-1 λ^4 ,2 λ^3 -benzo[4,5]thiazolo[3,2-c][1,3,5,2]oxadiazaborinin-3-yl)-N,N-dimethylaniline (**BFBB-4**). The reaction of *N*-(benzo[*d*]thiazol-2-yl)-4-(dimethylamino)benzamide (297 mg, 1.0 mmol) afforded **BFBB-4** (186 mg, 54%) as a yellow solid; mp 239–240 °C. ^1H NMR (400 MHz, CDCl_3): δ 8.25 (d, $J = 9.2$ Hz, 2H), 7.97 (d, $J = 8.4$ Hz, 1H), 7.73 (d, $J = 7.6$ Hz, 1H), 7.54 (t, $J = 8.0$ Hz, 1H), 7.41 (t, $J = 8.0$ Hz, 1H), 6.69 (d, $J = 9.2$ Hz, 2H), 3.12 (s, 6H) ppm; ^{13}C NMR (100 MHz, CDCl_3): δ 174.0, 168.6, 154.9, 140.6, 133.2 ($\times 2$), 128.1, 126.8, 125.8, 122.1, 118.2, 117.3, 111.2 ($\times 2$), 40.2 ppm; ^{19}F NMR (470 MHz, CDCl_3): δ -137.39 (d, $J = 11.2$ Hz), -137.45 (d, $J = 11.2$ Hz); IR (KBr): ν_{\max} 3458, 2952, 1618, 1554, 1462, 1425, 1405, 1371, 1194, 1124, 1043, 929, 823, 761 cm^{-1} ; LRMS (ESI+): m/z calcd for $\text{C}_{16}\text{H}_{15}\text{BF}_2\text{N}_3\text{OS}$ $[\text{M}+\text{H}]^+$ 346.1; found 346.1.

3. Photophysical properties

3.1 Absorbance spectra

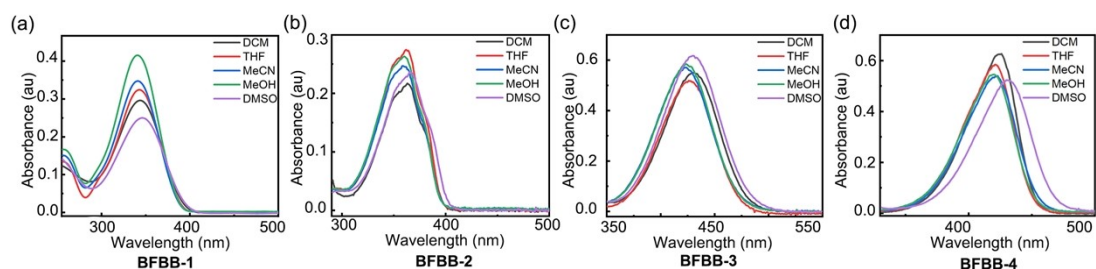


Fig. S1 UV-Vis spectra of **BFBB-1-4** (a-d) in different organic solvents. (**[1 and 3]** = 1×10^{-5} M, **[2]** = 5×10^{-6} M, and **[4]** = 1×10^{-6} M)

3.2 Fluorescence spectra

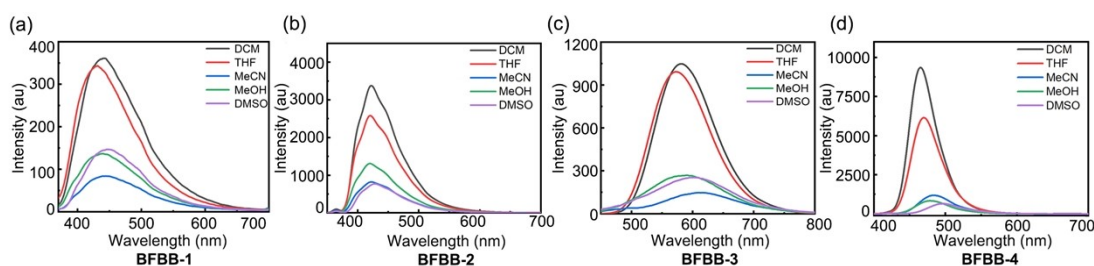


Fig. S2 PL spectra of **BFBB-1-4** (a-d) in different organic solvents. (**[1 and 3]** = 1×10^{-5} M and **[2 and 4]** = 1×10^{-6} M)

3.3 Absorbance and fluorescence spectra in solution and solid state

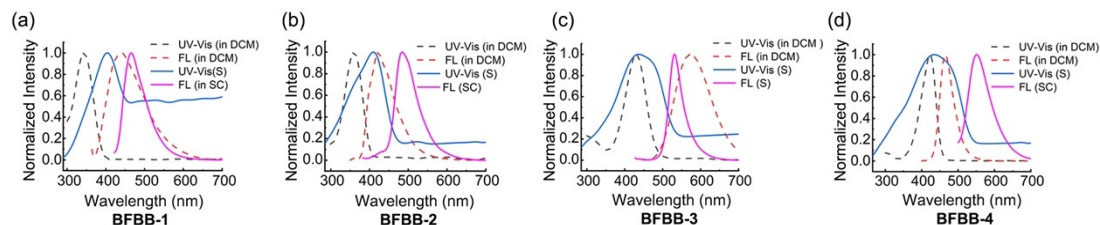


Fig. S3 UV-Vis and PL spectra of **BFBB-1-4** samples in CH_2Cl_2 and solid state. ((S): amorphous solid; (SC): single crystal))

3.4 DSE properties of BFBB-2

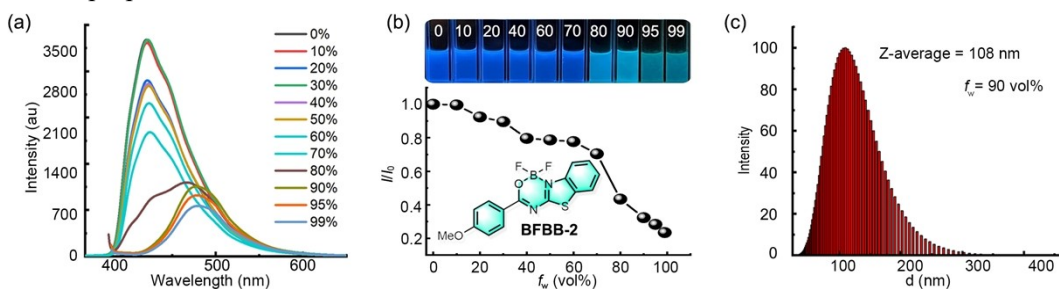


Fig. S4 (a) PL spectra of **BFBB-2** in MeCN and water/MeCN mixtures with different water fractions; (b) plots of I/I_0 value vs water fraction and photographs of **BFBB-2** in different water fractions taken under 365 nm UV light;

(c) DLS of **BFBB-2** in 90% water/MeCN mixture.

3.5 DSE properties of **BFBB-3**

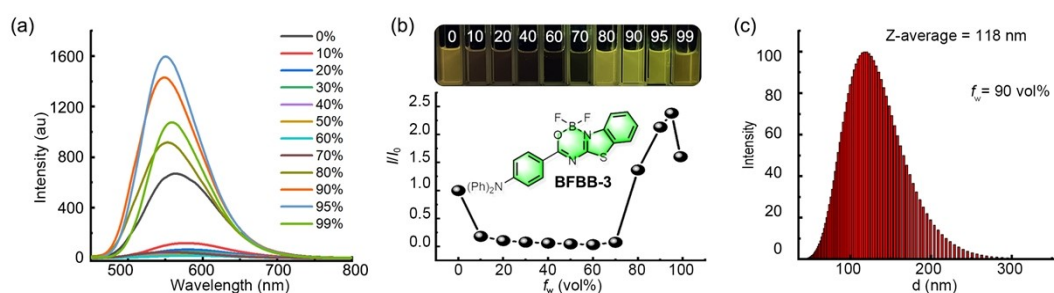


Fig. S5 (a) PL spectra of **BFBB-3** in MeCN and water/MeCN mixtures with different water fractions; (b) plots of I/I_0 value vs water fraction and photographs of **BFBB-3** in different water fractions taken under 365 nm UV light; (c) DLS of **BFBB-3** in 90% water/MeCN mixture.

4. Theoretical calculations

4.1 Vertical excitation of **BFBB-1-4**

Table S1 Selected parameters for the vertical excitation of **BFBB-1**

Electronic transition	Energy, eV/ λ nm	f^a	Composition ^b	CI ^c	Contribution
$S_0 \rightarrow S_1$	3.59/345	1.0089	H \rightarrow L	0.70459	99%
$S_0 \rightarrow S_2$	3.95/313	0.0283	H-1 \rightarrow L	0.69833	98%
$S_0 \rightarrow S_3$	4.15/299	0.0236	H-2 \rightarrow L	0.69163	96%
$S_0 \rightarrow S_4$	4.59/270	0.1638	H-3 \rightarrow L	0.68819	95%

Table S2 Selected parameters for the vertical excitation of **BFBB-2**

Electronic transition	Energy, eV/ λ nm	f^a	Composition ^b	CI ^c	Contribution
$S_0 \rightarrow S_1$	3.44/360	1.2160	H \rightarrow L	0.70315	99%
$S_0 \rightarrow S_2$	4.05/306	0.0276	H-2 \rightarrow L	0.52048	54%
			H-1 \rightarrow L	0.46107	43%
			H-2 \rightarrow L	-0.44922	41%
$S_0 \rightarrow S_3$	4.18/296	0.0033	H-3 \rightarrow L	-0.18580	6.9%
			H-1 \rightarrow L	0.49662	49.3%
$S_0 \rightarrow S_4$	4.36/284	0.0087	H-3 \rightarrow L	0.64570	83.3%
			H-2 \rightarrow L	-0.11753	2.8%
			H-1 \rightarrow L	0.14641	4.3%

Table S3 Selected parameters for the vertical excitation of **BFBB-3**

Electronic transition	Energy, eV/ λ nm	f^a	Composition ^b	CI ^c	Contribution
$S_0 \rightarrow S_1$	2.78/444	1.2257	H \rightarrow L	0.70192	99%
$S_0 \rightarrow S_2$	3.79/327	0.3096	H-1 \rightarrow L	0.69437	96%
$S_0 \rightarrow S_3$	3.94/314	0.0253	H-4 \rightarrow L	-0.18271	77%
			H \rightarrow L+1	0.64941	6.8%

			H→L+2	0.12128	2.9%
S ₀ →S ₄	4.05/306	0.0239	H-2→L	0.69214	96%

Table S4 Selected parameters for the vertical excitation of **BFBB-4**

Electronic transition	Energy, eV/λ nm	f^a	Composition ^b	CI ^c	Contribution
S ₀ →S ₁	3.05/406	1.3183	H→L	0.70091	98%
S ₀ →S ₂	4.01/309	0.0857	H-1→L	0.68512	94%
			H→L+2	0.11572	2.7%
S ₀ →S ₃	4.15/299	0.0225	H-2→L	0.68437	94%
			H→L+1	0.12368	3.1%
S ₀ →S ₄	4.30/288	0.0020	H-3→L	0.58878	69%
			H→L+2	0.21109	17.8%
			H→L+3	-0.31478	19.8%

^aOscillator strength. ^bH, HOMO (highest occupied molecular orbital) and L, LUMO (lowest unoccupied molecular orbital). ^cCoefficient of wavefunction.

4.2 MECI of **BFBB-1**

Table S5 Coordinates of the MECI of **BFBB-1**

	X	Y	Z
C	4.8341	0.80473	-0.9011
C	3.55161	0.98014	-0.41888
C	2.80423	-0.10522	0.02301
C	3.33169	-1.3966	-0.15393
C	4.61395	-1.56603	-0.65467
C	5.3707	-0.47018	-1.02795
H	5.42101	1.66447	-1.18507
H	3.13152	1.96719	-0.32254
H	2.75979	-2.24938	0.16704
H	5.02517	-2.55952	-0.73647
H	6.37151	-0.60413	-1.40649
C	1.40983	0.09306	0.398
N	0.70771	-1.15446	0.96135
C	-0.47369	-0.99581	0.65429
N	-0.96033	0.25961	0.15345
O	1.1059	1.14763	1.19549
B	-0.15445	1.6766	0.83812
F	-0.95644	2.01188	1.87479
F	-0.19036	2.57811	-0.18208
S	-1.81491	-2.19694	0.75929
C	-2.17597	0.18497	-0.29933
C	-2.8824	1.26983	-0.89859
C	-2.80946	-1.10722	-0.15079
C	-4.13354	1.03649	-1.37595
H	-2.38066	2.21768	-0.97778

C	-4.08057	-1.30605	-0.63804
C	-4.72908	-0.24016	-1.24907
H	-4.68502	1.82683	-1.8553
H	-4.57317	-2.25648	-0.52833
H	-5.72785	-0.3857	-1.62515

4.3 PL mechanism of **BFBB-2** and **4** in solutions

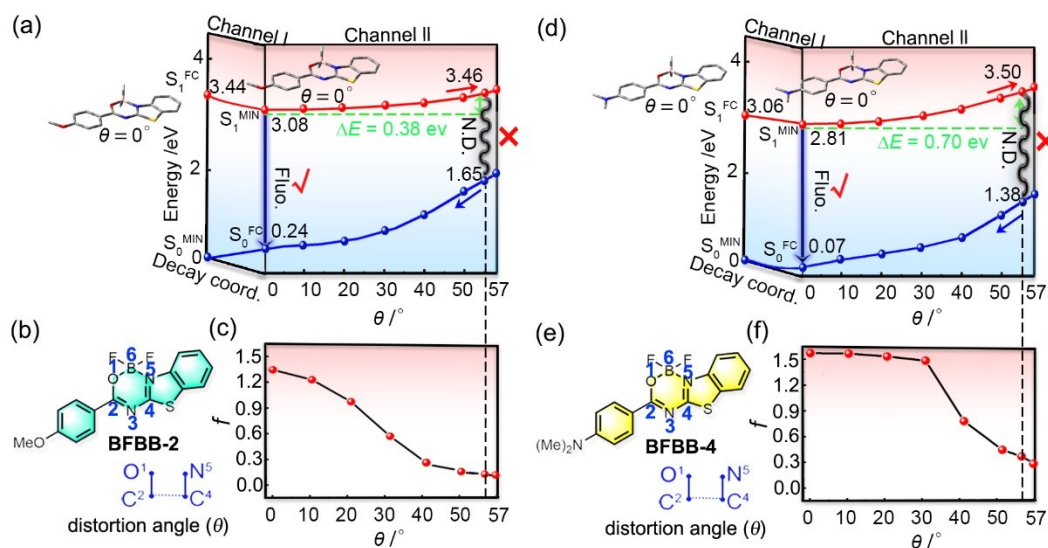


Fig. S6 Illustration of the nonradiative decay pathway in the two-channel model of **BFBB-2** (a) and **4** (d) in solutions. Distortion angle of **BFBB-2** (b) and **4** (e). Plot of f vs θ of **BFBB-2** (b) and **4** (e). (Fluo.: Fluorescence; N.D.: Nonradiative decay)

4.4 PL mechanism of **BFBB-1**, **2** and **4** in solid state

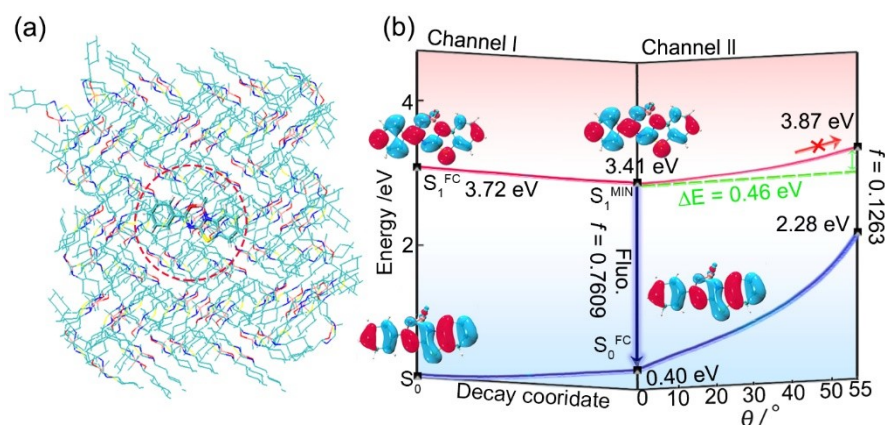


Fig. S7 Setup of the QM/MM model for **BFBB-1** (a). Illustration of the nonradiative decay pathway in the two-channel model of **BFBB-1** in solid state (b). Insets: Molecular orbital amplitude plots of HOMO and LUMO and the corresponding oscillator strengths.

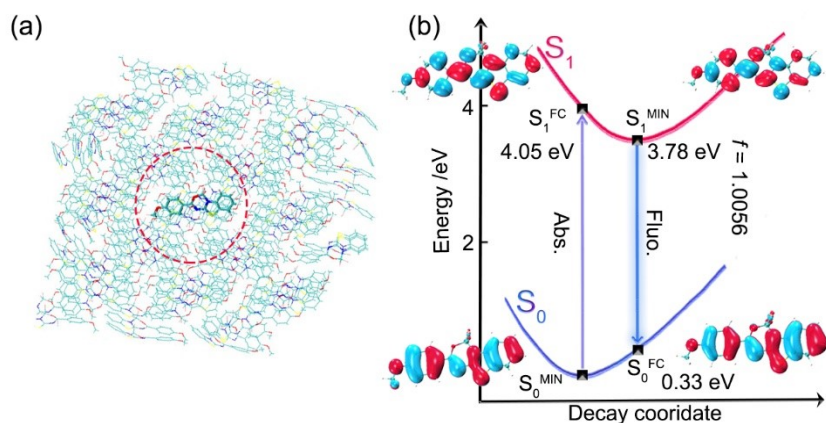


Fig. S8 Setup of the QM/MM model for **BFBB-2** (a). Optimized S_1^{FC} - and S_1^{MIN} -state geometries of **BFBB-2** in solid state (b). Insets: Molecular orbital amplitude plots of HOMO and LUMO and the corresponding oscillator strength.

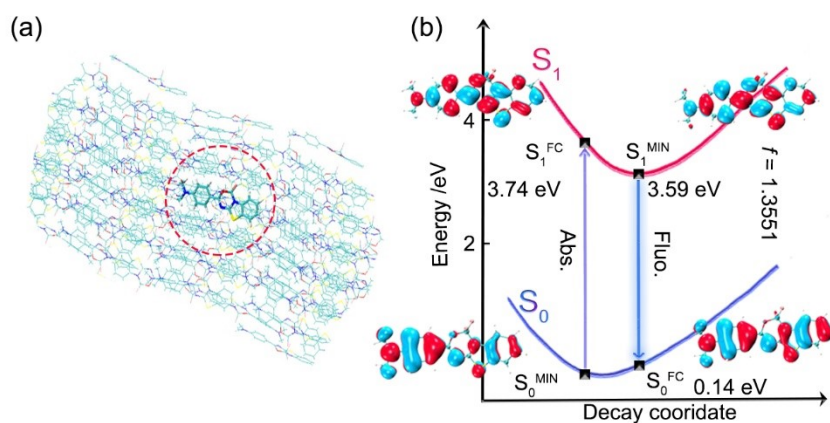
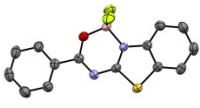
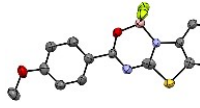
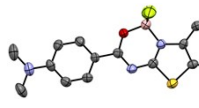


Fig. S9 Setup of the QM/MM model for **BFBB-4** (a). Optimized S_1^{FC} - and S_1^{MIN} -state geometries of **BFBB-4** in solid state (b). Insets: Molecular orbital amplitude plots of HOMO and LUMO and the corresponding oscillator strength.

5. Crystallographic analysis

5.1 Single crystal data

Table S6 ORTEP drawings, CCDC numbers, and crystal data of **BFBB-1**, **2**, and **4**

	 BFBB-1	 BFBB-2	 BFBB-4
CCDC Number	2295395	2295401	2295402
Formula	C ₁₄ H ₉ BF ₂ N ₂ OS	C ₁₅ H ₁₁ BF ₂ N ₂ O ₂ S	C ₁₇ H ₁₄ BF ₂ N ₂ OS
Formula weight	302.10	332.13	345.47
Temperature (K)	296(2)	296(2)	296(2)
Crystal system	Orthorhombic	Triclinic	Triclinic
Space group	P21/n	P-1	P-1
Unit cell dimensions			
a (Å)	8.8226(6)	7.1570(10)	7.9897(8)
b (Å)	11.55942(9)	15.2480(7)	11.3528(11)
c (Å)	25.3522(18)	13.6954(14)	34.408(3)
α (°)	90	90	90
β (°)	90	105.1090(10)	89.989(2)
γ (°)	90	90	90
Volume (Å ³)	2593.3(3)	1442.9(3)	3121.0(5)
Z	25	4	2
Density(calcd)(g/cm ³)	1.548	1.129	1.470
Goodness-of-fit on F ²	1.039	1.129	1.018
Final R indices[I/2σ(I)]			
R ₁	0.0338	0.4757	0.0731
w R ₂	0.0790	0.4905	0.1977
R indices (all data)			
R ₁	0.0401	0.2128	0.1473
w R ₂	0.0821	0.1865	0.1594

5.2 Slicing of the 3D crystal structures

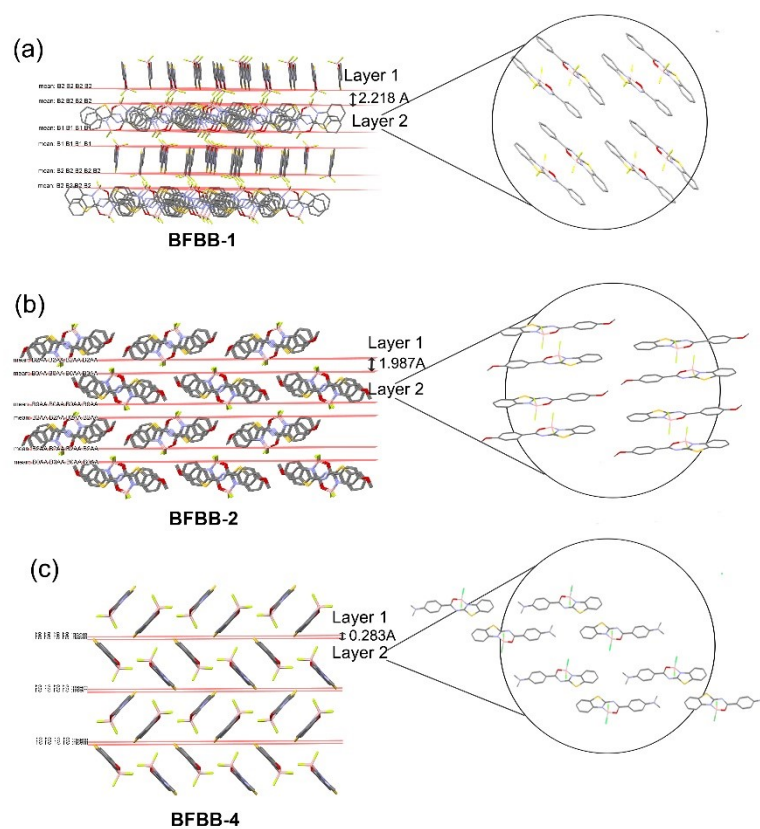


Fig. S10 The staggered stacking mode of layers in the single crystals of **BFBB-1** (a), **2** (b), and **4** (c).

6. NMR spectra

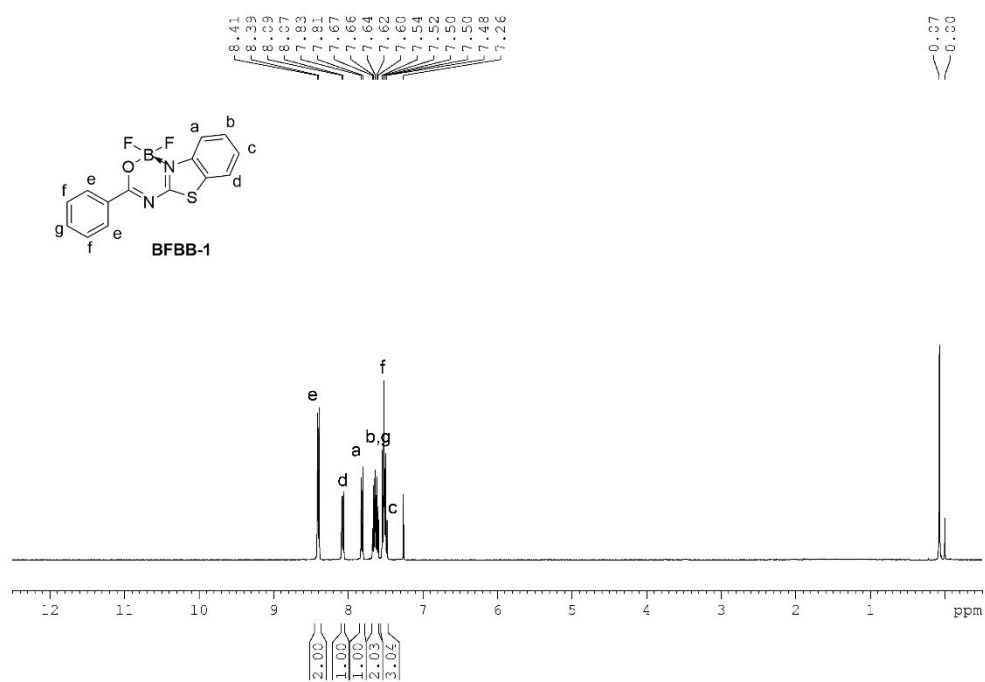


Fig. S11 ¹H NMR spectrum of BFBB-1

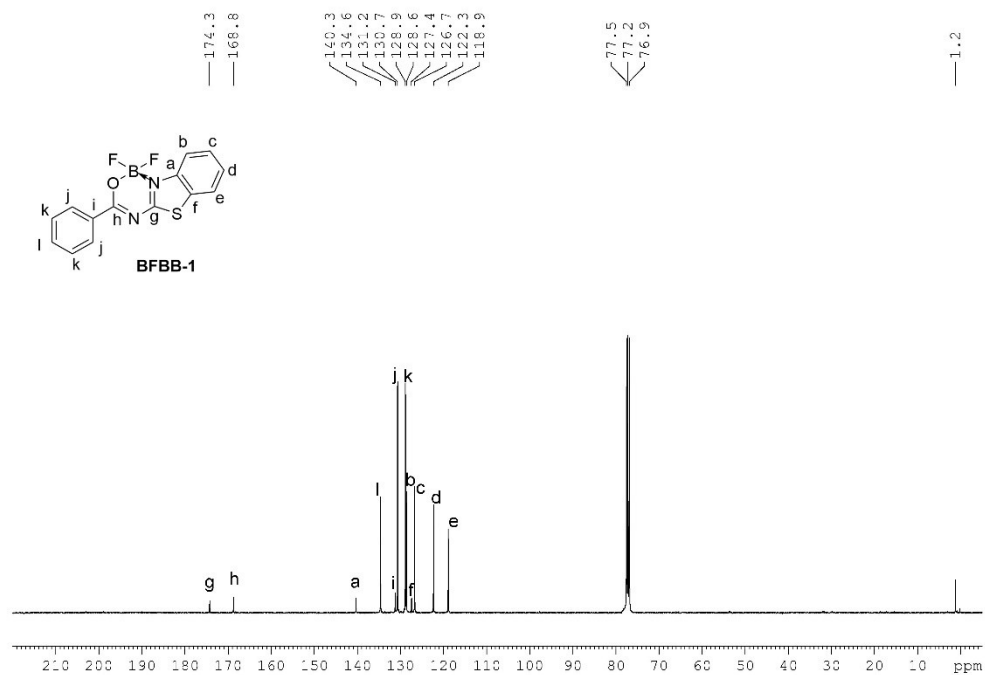


Fig. S12 ¹³C NMR spectrum of BFBB-1

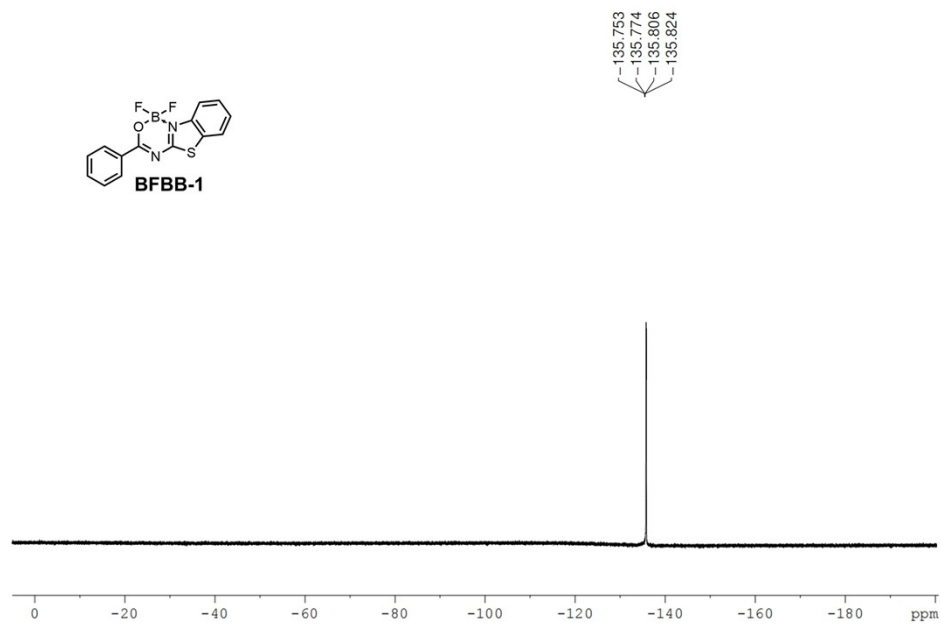


Fig. S13 ^{19}F NMR spectrum of BFBB-1

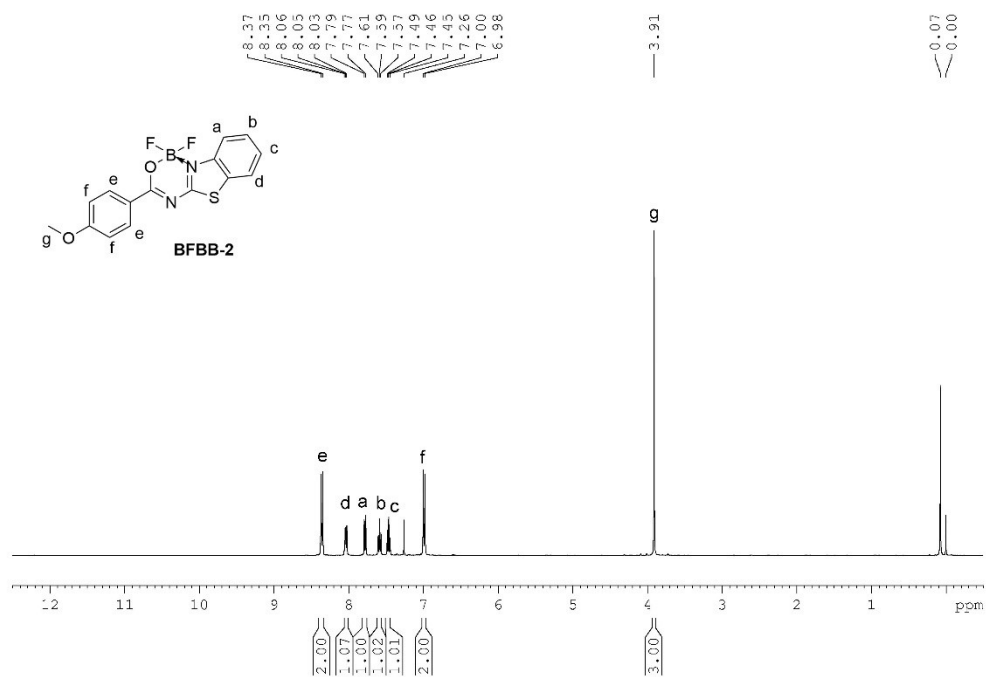


Fig. S14 ^1H NMR spectrum of BFBB-2

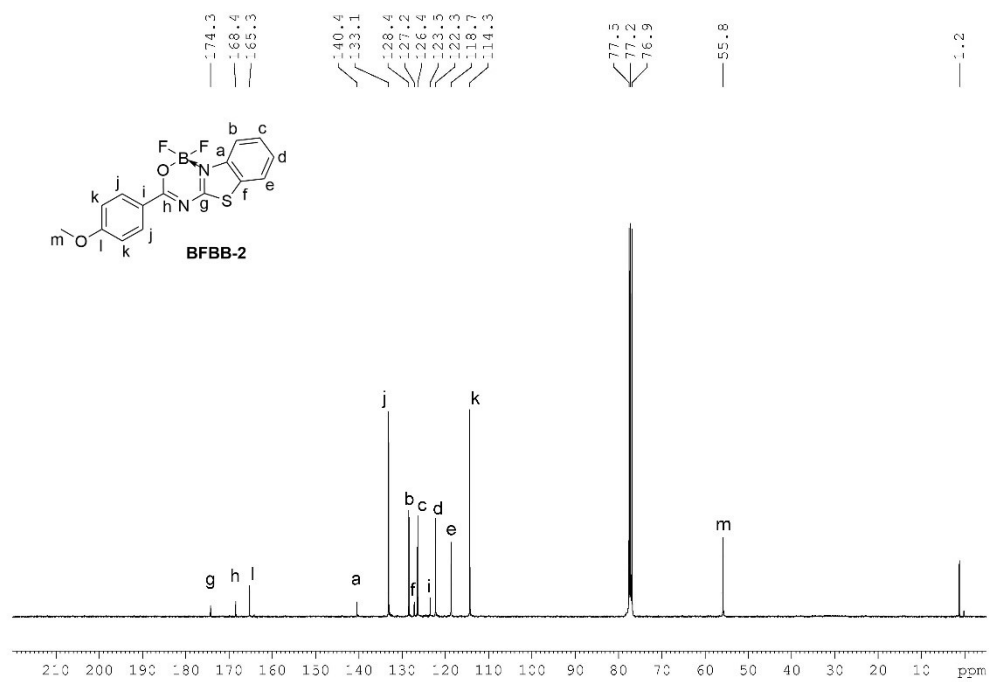


Fig. S15 ^{13}C NMR spectrum of **BFBB-2**

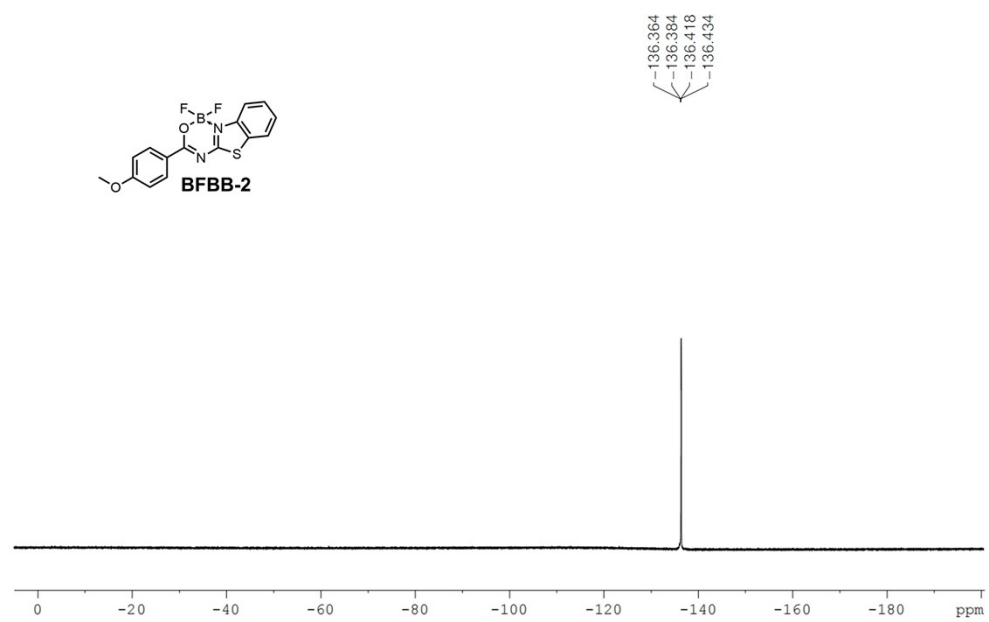


Fig. S16 ^{19}F NMR spectrum of **BFBB-2**

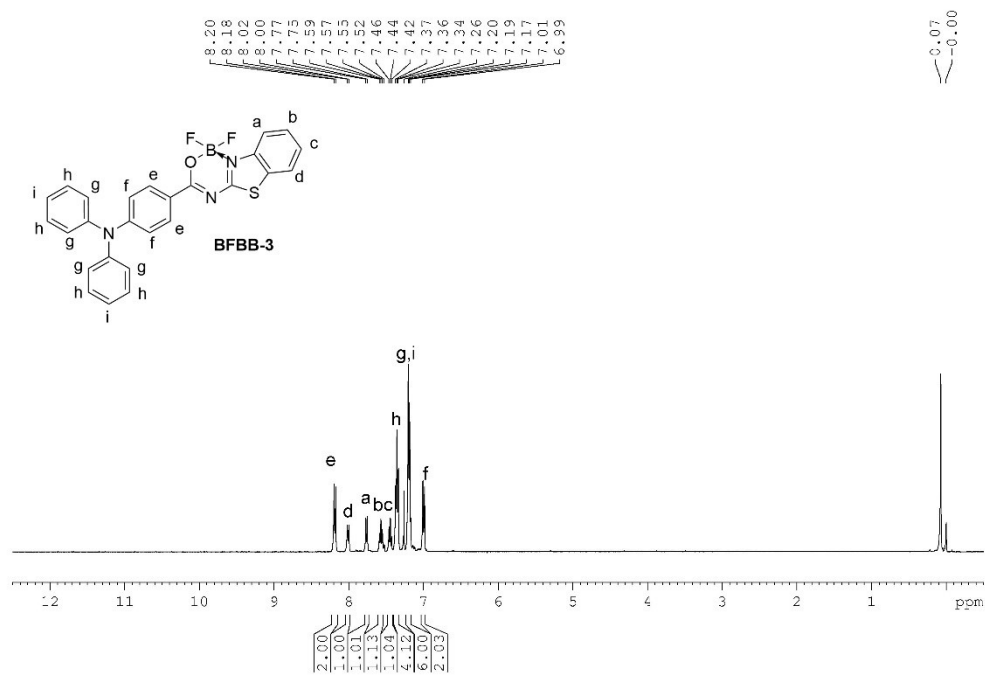


Fig. S17 ¹H NMR spectrum of **BFBB-3**

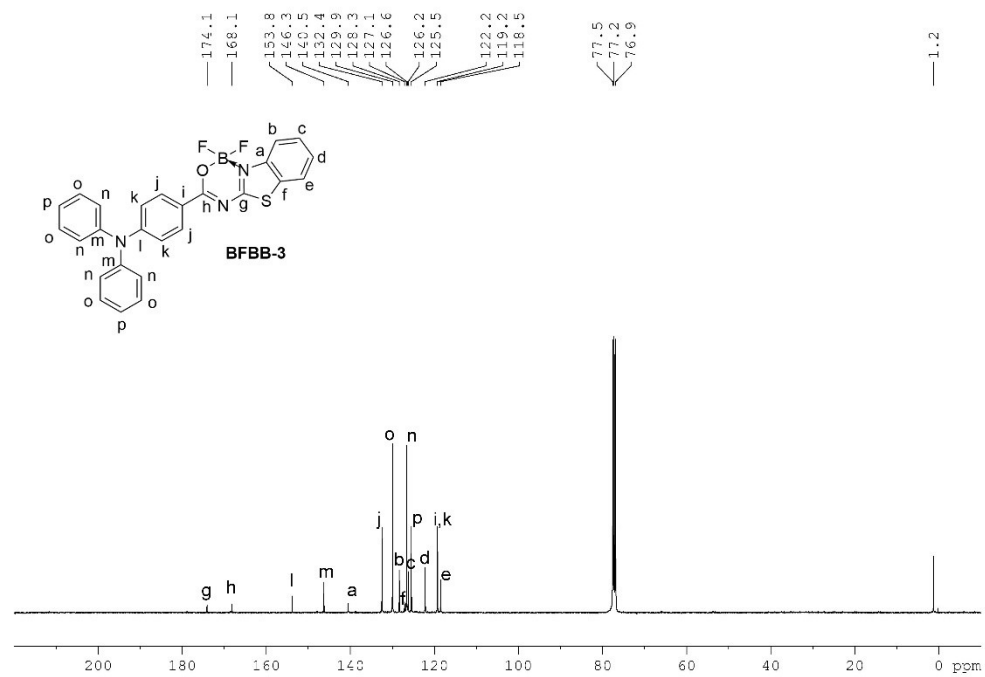


Fig. S18 ¹³C NMR spectrum of **BFBB-3**

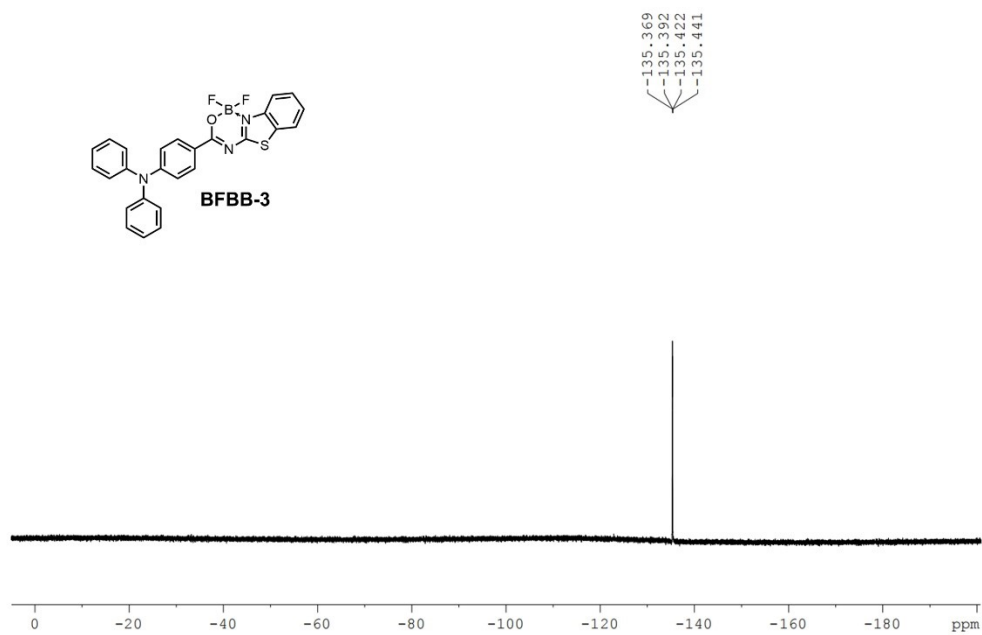


Fig. S19 ^{19}F NMR spectrum of **BFBB-3**

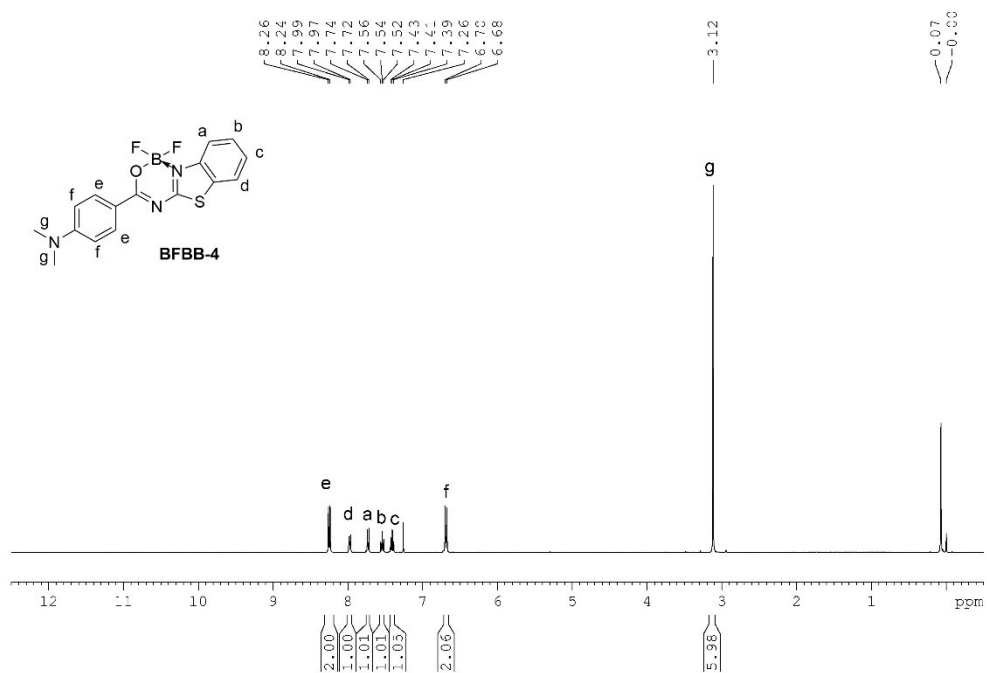


Fig. S20 ^1H NMR spectrum of **BFBB-4**

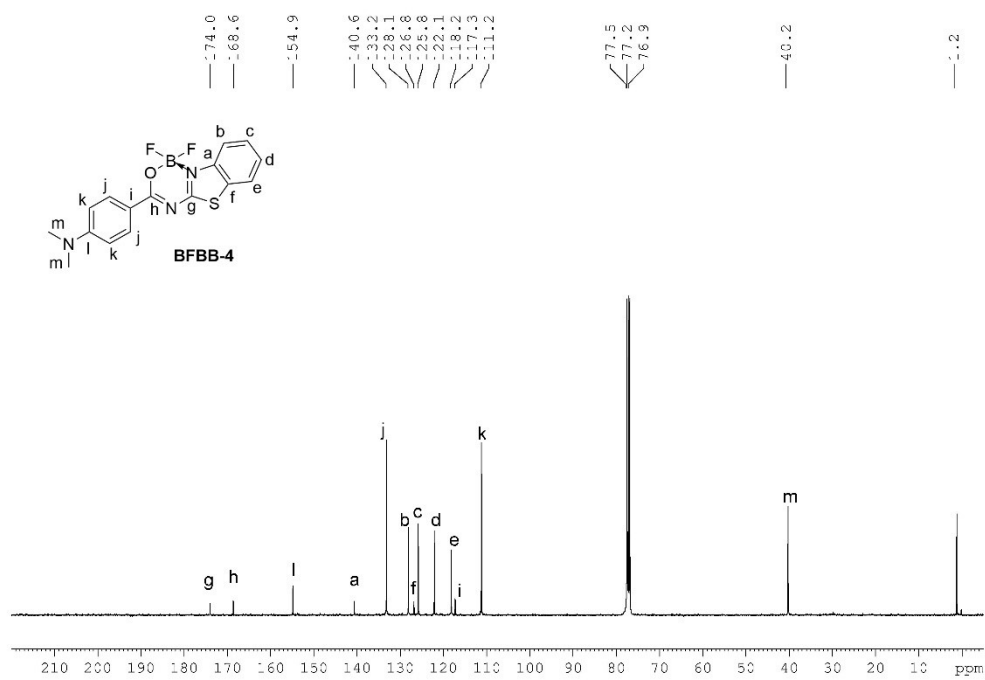


Fig. S21 ¹³C NMR spectrum of BFBB-4

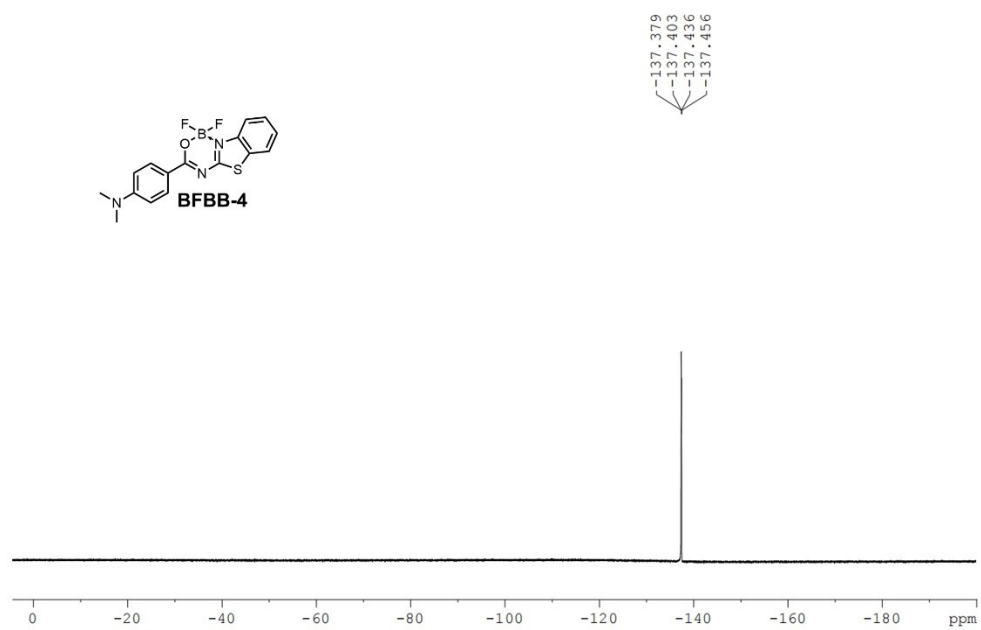


Fig. S22 ¹⁹F NMR spectrum of BFBB-4